Control of Andreev-level occupation in a Josephson junction by a normal-metal probe

Li-Fu Chang and Philip F. Bagwell
School of Electrical and Computer Engineering, Purdue University, West Lafayette, Indiana 47907
(Received 31 October 1996)

We calculate the electrical current flowing through a mesoscopic superconductor–normal-metal–superconductor (SNS) junction coupled to a normal-metal probe. This additional normal terminal models either a scanning tunneling microscope probe or the gate electrode of a three-terminal SNS junction. We find the Josephson current switches between two different values as the probe voltage V is varied. This switching occurs because the Andreev energy levels are populated with an effective electrochemical potential eV. When the probe voltage $|eV|>\Delta$, so that all of the Andreev levels are either filled or emptied, we show it is possible to directly measure the ''continuum'' contribution to the Josephson current. The differential conductance dI/dV at the normal probe can also be used to detect the density of Andreev levels. [S0163-1829(97)09417-4]

I. INTRODUCTION

Additional leads or ''probes'' attached to a conductor have long been employed in normal mesoscopic systems both to control the energy-level occupation and to introduce quantum-mechanical phase breaking.[1,2]. In normal mesoscopic systems, the occupation of an energy level is determined primarily by the probe with the strongest coupling to that level. But the situation is somewhat different for electrons trapped in the Andreev energy levels[3] of a Josephson junction.[4–8] As pointed out in Ref. 7, quasiparticles incident from a superconducting reservoir cannot elastically scatter into an Andreev level. In order to populate the Andreev levels, Ref. 7 introduced an additional normal-metal probe coupled to the normal region of a superconductor–normal-metal–superconductor (SNS) junction as shown in Fig. 1. Even though quasiparticles can travel ballistically into the strongly coupled superconducting leads, and must pass through a tunnel barrier to enter the weakly coupled normal-metal lead, Ref. 7 shows it is the normal-metal probe which controls the bound Andreev-level occupation.

In this paper we employ the Bogoliubov–de Gennes (BdG) equation[9] to calculate the electrical currents through the SNS junction shown in Fig. 1. An additional normal-metal probe is attached to the N region of the SNS junction, following Ref. 7. The two superconducting leads are held at zero voltage, while the normal lead is biased at a voltage V. To describe the coupling of the normal-metal probe to the SNS junction, we use a scattering matrix which forces the quasiparticle to turn into the side probe[1,2] with probability ϵ. We compute both the current flow into the superconducting leads and the current flow into the normal-metal lead as a function of the macroscopic phase difference ϕ between the two superconductors, the voltage V, and the coupling strength ϵ to the normal-metal lead.

Using a normal-metal side probe to control the Andreev-level occupation also controls the Josephson current. In SNS junctions shorter than the coherence length ($L \ll \xi_0$), and for a weakly coupled normal-metal probe ($\epsilon \to 0$), we find the Josephson current switches abruptly to zero at a certain voltage $|eV| \leqslant \Delta$ and remains zero for $|eV| \geqslant \Delta$. This single switching event occurs when the probe voltage V forces the two Andreev levels in a short SNS junction to both be populated (or depopulated). Once the Andreev levels are filled (or emptied), and therefore carry no net current, the total Josephson current in the short SNS junction is also forced to zero.

When the normal-metal probe is weakly coupled ($\epsilon \to 0$) to a long SNS junction ($L \gg \xi_0$), we show the Josephson current switches between two values as function of V for $|eV| \leqslant \Delta$. The Josephson current switching for $|eV| \leqslant \Delta$ again arises from the population (or depopulation) of bound Andreev levels inside the superconducting energy gap. The change in the current after populating (or depopulating) a new Andreev level we find to be $\Delta I \simeq e v_F/(L+2\xi_0)$. Whenever the Josephson current switches, i.e., when the electrochemical potential eV of the normal lead crosses a new An-

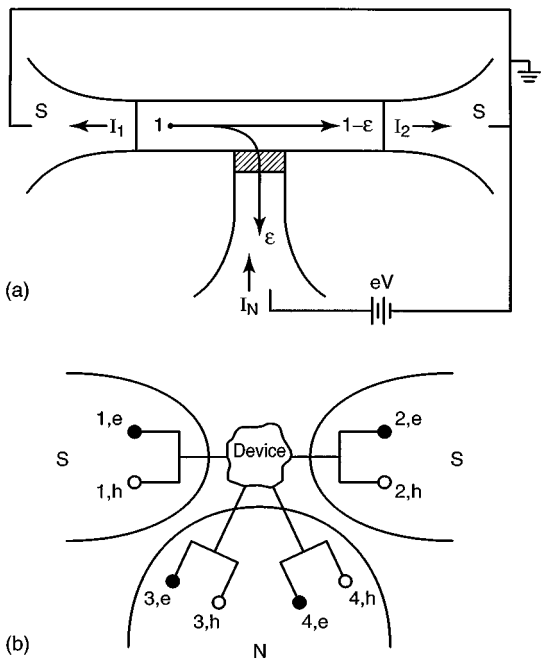

FIG. 1. (a) Geometry of an SNS junction coupled to a normal-metal probe. The probe is biased at $\mu_N = eV$, while the superconducting leads are grounded. (b) Mathematical configuration of leads needed to represent the SNS junction.

dreev level, the differential conductance dI_N/dV along the normal-metal lead also has a peak. The density of levels in the SNS junction can therefore be detected by measuring the differential conductance dI_N/dV along the normal metal lead.

The continuum of energy levels outside the superconducting energy gap also contribute to the Josephson current in a long SNS junction. It should be possible to directly measure this ''continuum'' contribution to the Josephson current by attaching a weakly coupled normal-metal probe ($\epsilon \to 0$) to a long Josephson junction. When the side probe voltage exceeds the superconducting gap ($|eV| \geq \Delta$), so that the Andreev levels are either completely filled or emptied, we find the total current carried inside the superconducting energy gap is nearly zero. This leaves only the energy continuum available to contribute to the Josephson current. Since the continuum energy levels are more strongly coupled to the superconducting leads than to the normal lead, so that their occupation is nearly independent of the voltage applied to the normal-metal lead, we find this continuum current flow into the superconductors is nearly constant as a function of V when $|eV| \geq \Delta$. The energy distribution of the Josephson current between the discrete energy levels inside the gap and the continuum of energy levels outside the gap can therefore be directly measured as the terminal current flowing into one of the superconductors.

II. MODEL FOR THE GATED SNS JUNCTION

We describe quasiparticle motion in the SNS junction of Fig. 1 by the BdG equation

$$\begin{pmatrix} H(x)-\mu & \Delta(x) \\ \Delta^*(x) & -(H^*(x)-\mu) \end{pmatrix} \begin{pmatrix} u(x) \\ v(x) \end{pmatrix} = E \begin{pmatrix} u(x) \\ v(x) \end{pmatrix}, \quad (1)$$

where the one-electron Hamiltonian is $H(x) = -(\hbar^2/2m)(d^2/dx^2)$. We model the SNS junction by a step change of the superconducting order parameter, namely

$$\Delta(x) = \begin{cases} \Delta e^{i\phi_1}, & x < 0, \\ 0, & 0 < x < L, \\ \Delta e^{i\phi_2}, & x > L. \end{cases} \quad (2)$$

This model for the pair potential $\Delta(x)$ is justified because the narrow portion of the conductor widens into two bulk superconductors, which can be regarded as order parameter reservoirs.[5]

The motion of electrons and holes in the normal region ($0 < x < L$) is modified by coupling them to a normal-metal probe (at $x = a$) as shown in Fig. 1(a). The quasiparticle waves in the side probe are also described by Eq. (1) with $x \to y$ and $\Delta(y) = 0$. We use a parameter ϵ to describe the coupling strength to the external probe. As outlined in Appendix A, a right-moving electron in the normal region in Fig. 1(a) has a probability ϵ of leaking into the normal lead. For $\epsilon = 0$ the SNS junction and the normal conductor are decoupled, while for $\epsilon = 1$ the quasiparticle phase coherence (necessary to establish the Josephson effect) has been completely broken. Because we wish to attach a normal-metal probe which only breaks the electron phase, but not its momentum, it is necessary to attach two ''conceptual'' normal-metal probes for each physical normal probe.[1,2] These additional conceptual leads are labeled as channels 3 and 4 in Fig. 1(b). For the type of side-probe considered in Ref. 7, which breaks both momentum and phase of the quasiparticles, the additional channel 4 is unnecessary.

As shown in Ref. 10, the standard Landauer-Büttiker formalism for electrical transport in multiterminal mesoscopic normal conductors applies directly to mesoscopic superconductors, provided we replace every lead with by a separate conceptual lead for electron and hole quasiparticles. We use the indices $p,q = 1,2,3,4$ as the lead numbers and n is the quantum number of the injected state. We typically have $n = (k, \beta)$, where k is the wave number of the injected state and $\beta = (e \text{ or } h)$ denotes the injection of electronlike or holelike quasiparticles. We therefore calculate the electrical current flow in lead p due to injection of a quasiparticle in the qn channel according to[10,11]

$$I_p = \sum_{qn} (J_u + J_v)_{p;qn} f_{qn} - \sum_{qn} (J_v)_{p;qn}. \quad (3)$$

The Schrödinger currents associated with the waves u and v from Eq. (1) are $J_u = (e\hbar/m)\mathrm{Im}\{u^*(x)\nabla u(x)\}$ and $J_v = (e\hbar/m)\mathrm{Im}\{v^*(x)\nabla v(x)\}$. The ''vacuum current'' due to the filled hole band is argued in Ref. 10 to be zero, namely $\Sigma_{qn}(J_v)_{p;qn} = 0$. The electrical current in Eq. (3) is related to a transmission coefficient $\tilde{T}$ by

$$(J_u + J_v)_{p;qn} = \tilde{T}_{p;qn} = e v_p T_{p;qn}, \quad (4)$$

where $v_p = \hbar k_p/m$. Equation (3) then reduces to the standard Landauer-Büttiker form familiar from normal mesoscopic electron transport, namely,

$$I_p = e \sum_{qn} v_p T_{p;qn} f_{qn}. \quad (5)$$

The Fermi factor f_{qn} in Eq. (5) must be calculated properly to obtain the correct electrical current. As also shown in Ref. 10, the Fermi factors are different for injected electronlike and holelike quasiparticles, namely,

$$f_{qn} = f_{q\beta} = f(E - eV_{q\beta}), \quad (6)$$

where the Fermi function is $f(E) = 1/[1 + \exp(E/k_B T)]$. The effective biasing voltage $eV_{q\beta}$ applied to the $(q\beta)$th lead is contained in the Fermi factor in Eq. (3). The bias applied to the normal-metal lead produces the effective electrochemical potentials[10]

$$V_{3e} = V_{4e} = V, \quad (7)$$

$$V_{3h} = V_{4h} = -V. \quad (8)$$

In this paper the superconducting leads are grounded so that $eV_{1\beta} = eV_{2\beta} = 0$. Considering only the case where the superconductors are both grounded greatly simplifies calculation,

as the addition of a bias on either superconducting lead requires the use of time-dependent BdG equations.[12]

We apply Eq. (5) to calculate the electrical currents $I_1(\phi,\epsilon,V)$ in the left superconductor, $I_2(\phi,\epsilon,V)$ in the right superconductor, and $I_N(\phi,\epsilon,V)=I_3(\phi,\epsilon,V)+I_4(\phi,\epsilon,V)$ in the normal lead, shown in Fig. 1(a). As detailed in Appendix B, we obtain for the current flowing into the left superconductor

$$-I_1(\phi,\epsilon,V)=\frac{2e\epsilon}{h}\int_{-\Delta}^{\Delta}\tanh\left(\frac{E-eV}{2k_BT}\right)\left(\frac{1}{F(E,\epsilon,\phi)}-\frac{1-\epsilon}{F(E,\epsilon,-\phi)}\right)dE+\frac{e\epsilon}{h}\left(\int_{-\infty}^{-\Delta}+\int_{\Delta}^{\infty}\right)\tanh\left(\frac{E-eV}{2k_BT}\right)$$
$$\times\left(\frac{u_0^2}{D(E,\epsilon,\phi)}-\frac{(1-\epsilon)v_0^2}{D(E,\epsilon,-\phi)}\right)dE+(2-\epsilon)\frac{e}{h}\int_{\Delta}^{\infty}\tanh\left(\frac{E}{2k_BT}\right)\frac{U(E,\epsilon)}{|u_0^2-v_0^2|}\left(\frac{1}{D(E,\epsilon,\phi)}-\frac{1}{D(E,\epsilon,-\phi)}\right)dE. \tag{9}$$

The current into the right superconductor we obtain from

$$I_2(\phi,\epsilon,V)=I_1(-\phi,\epsilon,V). \tag{10}$$

The current flowing out of the normal-metal lead we find to be

$$-I_N(\phi,\epsilon,V)=\frac{2e\epsilon^2}{h}\int_{-\Delta}^{\Delta}\tanh\left(\frac{E-eV}{2k_BT}\right)\left(\frac{1}{F(E,\epsilon,-\phi)}+\frac{1}{F(E,\epsilon,\phi)}\right)dE+\frac{e\epsilon}{h}\left(\int_{-\infty}^{-\Delta}+\int_{\Delta}^{\infty}\right)\tanh\left(\frac{E-eV}{2k_BT}\right)[u_0^2-(1-\epsilon)v_0^2]$$
$$\times\left(\frac{1}{D(E,\epsilon,-\phi)}+\frac{1}{D(E,\epsilon,\phi)}\right)dE. \tag{11}$$

In Eqs. (9)–(11) the function $D(E,\epsilon,\phi)$ is

$$D(E,\epsilon,\phi)=u_0^4+v_0^4(1-\epsilon)^2-2u_0^2v_0^2(1-\epsilon)\times\cos\left[\left(\frac{E}{\Delta}\right)\left(\frac{L}{\xi_0}\right)+\phi\right], \tag{12}$$

the function $F(E,\epsilon,\phi)$ is

$$F(E,\epsilon,\phi)=1+(1-\epsilon)^2-2(1-\epsilon)\times\cos\left[-2\cos^{-1}\left(\frac{E}{\Delta}\right)+\left(\frac{E}{\Delta}\right)\left(\frac{L}{\xi_0}\right)+\phi\right], \tag{13}$$

and the function $U(E,\epsilon)$ is

$$U(E,\epsilon)=u_0^4+v_0^4(1-\epsilon)-u_0^2v_0^2[(1-4v_0^2)\epsilon+2]. \tag{14}$$

The coherence factors u_0 and v_0 are

$$2u_0^2=1+\frac{\sqrt{E^2-\Delta^2}}{|E|}, \tag{15}$$

and

$$2v_0^2=1-\frac{\sqrt{E^2-\Delta^2}}{|E|}, \tag{16}$$

while the superconducting phase difference is $\phi=\phi_2-\phi_1$. Equations (9)–(11) satisfy $I_N=I_1+I_2$ as required for electrical current conservation.

Equations (9)–(11) describe how the multiple Andreev reflections between the two superconductors are modified by coupling to the normal-metal probe. When the normal probe and Josephson junction are completely decoupled, namely, $\epsilon=0$, the multiple Andreev reflections between the two superconductors produce bound Andreev levels inside the superconducting gap and weaker quasibound levels outside the gap.[8] These energy levels broaden as the coupling ϵ increases, and their filling begins to be controlled by the voltage on the normal-metal probe. This can be seen from the structure of Eqs. (9)–(11). Terms containing the occupation factor $\tanh[(E-eV)/2k_BT]$ are currents injected from the normal-metal lead, while terms with the occupation factor $\tanh[E/2k_BT]$ are currents injected from the superconducting contacts. By inspection of Eqs. (9)–(11) one immediately infers that currents flowing in the energy range $-\Delta\leqslant E\leqslant\Delta$, i.e., current flow through the broadened Andreev bound levels, are occupied by the Fermi factor of the normal-metal lead. How the Andreev levels broaden and shift in energy by coupling to the normal lead is determined by the poles of the first term in Eqs. (9)–(11), namely the complex energies at which $F(E,\epsilon,\phi)=0$, as described in Appendixes A and C.

III. CURRENT FLOW IN GATED SNS JUNCTION

A. Equilibrium current and phase breaking

We first consider the side probe shorted to the two superconductors so that $eV=0$. In this limit Eqs. (9)–(11) give $I_N=0$ and $I_1=-I_2$. The zero-temperature Josephson current $I_2(\phi)$ is then suppressed by quasiparticle phase breaking as shown in Figs. 2(a) and 2(b). For both (a) short ($L\ll\xi_0$) and (b) long ($L\gg\xi_0$) SNS junctions,[13] the current-phase relation $I_2(\phi)$ of the completely coherent ($\epsilon=0$) Josephson junction[8] is rounded into the standard Ambegaokar-

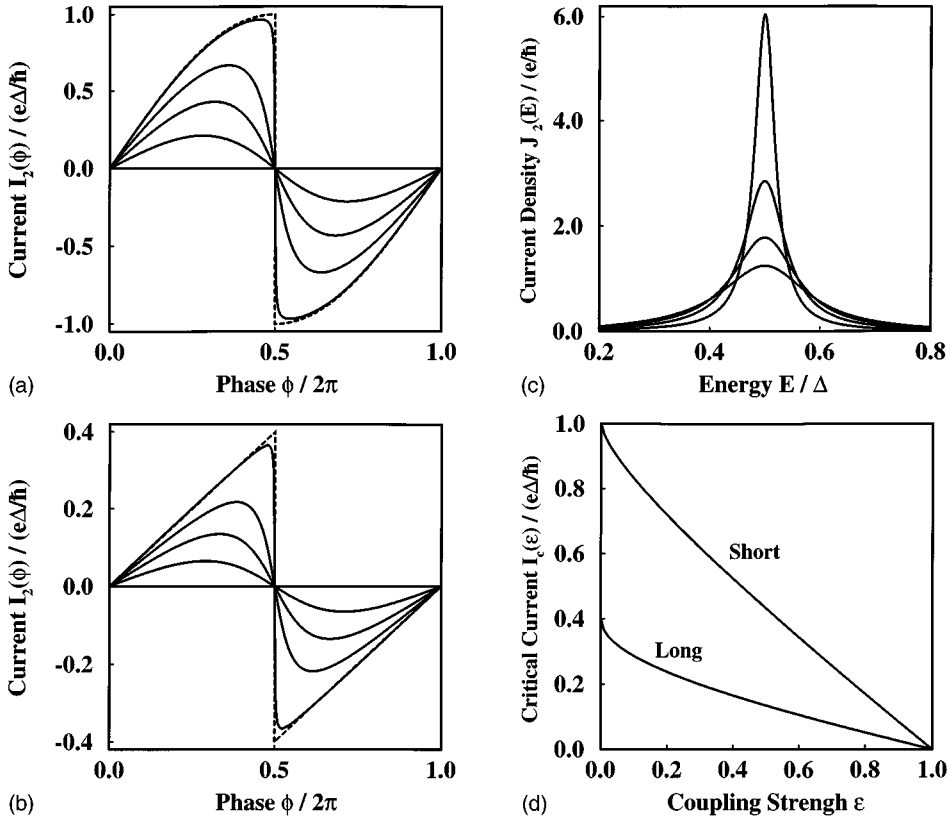

FIG. 2. The current-phase relation for a (a) short and (b) long SNS junction is rounded by quasiparticle phase breaking. The Andreev energy levels are broadened with increasing phase breaking, as shown by the (c) current density per unit energy $J_2(E)$ flowing through the Andreev energy level in a short junction. (d) The critical current also decreases as the phase-breaking parameter ϵ increases, for both short (top curve) and long (bottom curve) junctions.

Baratoff form $I=I_c\sin(\phi)$ as ϵ increases. The coupling to the side probe in Figs. 2(a) and 2(b) is $\epsilon=0$(dashed),1,25,50,75,100%.

Rounding of the current-phase relation into an Ambegaokar-Baratoff form is accompanied by a broadening of the Andreev energy levels, illustrated in Fig. 2(c) for a short SNS junction with $\phi=2\pi/3$. The probe coupling used in Fig. 2(c) is $\epsilon=5,10,15,20$ %. The electrical current density $J_2(E)$, where $I_2=\int_{-\infty}^{\infty}J_2(E)dE$, spreads out over a larger energy range as ϵ increases. The Andreev-level width is approximately $\epsilon(\hbar v_F)/(L+2\xi_0)$ for small ϵ, as obtained in Appendixes A and C. Both the bound Andreev levels and weak quasibound Andreev resonances in the scattering continuum are broadened by coupling to the normal-metal lead. The critical current is also suppressed with increasing coupling to the side probe as shown in Fig. 2(d) for both short (top) long (bottom) SNS junctions. As $\epsilon=1$, so that the quasiparticle phase is completely randomized, we find the critical current $I_c\rightarrow 0$.

B. Current-phase relation for weak coupling to the side probe

We now apply a voltage bias $eV>0$ to the normal lead. We consider first the case where the side probe is only weakly coupled to the SNS junction ($\epsilon=1\%$), so the current I_N is small. We plot the Andreev bound levels from the resonance condition[4]

$$-2\cos^{-1}\left(\frac{E}{\Delta}\right)+\left(\frac{E}{\Delta}\right)\left(\frac{L}{\xi_0}\right)\pm\phi=2\pi n, \qquad (17)$$

$n=0,\pm 1\pm 2\cdots$, in Fig. 3(a). The BCS healing length in Eq. (17) is $\xi_0=\hbar v_F/2\Delta$. The current I_2 flowing into the second superconductor from Eq. (10) is shown in Fig. 3(b), while the current I_N from Eq. (11) flowing out of the probe is plotted in Fig. 3(c). We see $I_N\ll I_2$, indicating a weakly coupled probe.

The electrical current flows only through the discrete energy levels of Fig. 3(a) in a short SNS junction, and the occupation of these discrete levels is controlled by the voltage V on the side probe. In Fig. 3(a) we have therefore drawn a dashed line corresponding to the bias voltage $eV=0.75\Delta$. The phase difference $\phi_0=2\cos^{-1}(E/\Delta)\simeq 0.46\pi$, where an Andreev level crosses the energy $E=eV$ corresponding to the bias voltage, is also shown by a vertical dot-dashed line in Fig. 3(a).

Since the probe voltage eV sets the effective electrochemical potential for the Andreev levels, any Andreev level having $E_n\leqslant eV$ in Fig. 3(a) is filled. When only one Andreev level is filled, that is when $\phi<\phi_0$, the electrical current is nearly the same as when the probe is not connected to the SNS junction. When both Andreev levels are occupied, that is for $\phi_0<\phi<(2\pi-\phi_0)$, the two levels carry equal and opposite electrical currents. Filling (or emptying) all the Andreev bound levels (by changing the voltage on the side probe) therefore forces the total current carried by the dis-

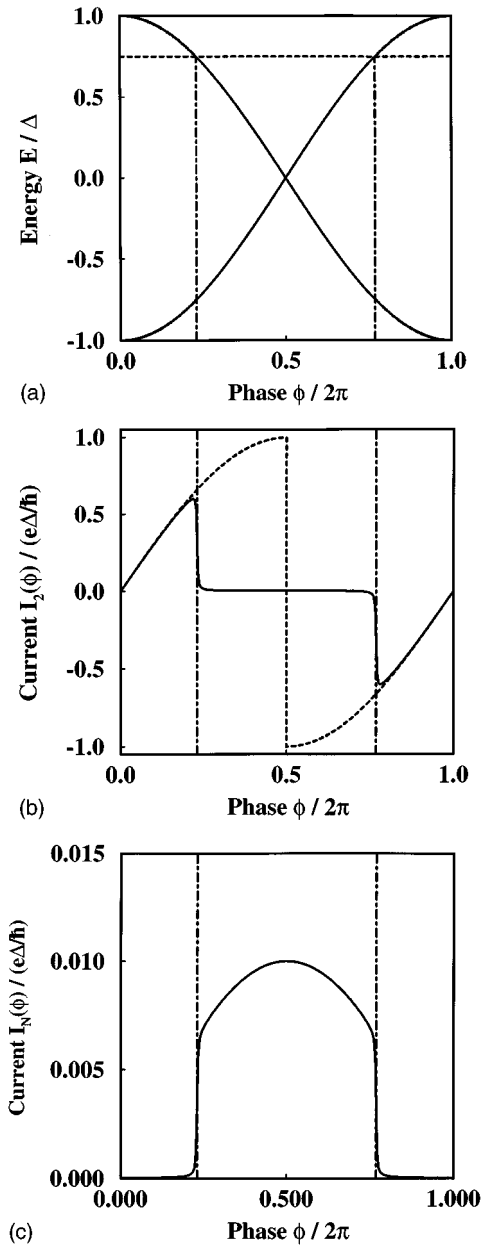

FIG. 3. (a) Andreev energy levels $E_n^{\pm}(\phi)$, (b) current $I_2(\phi)$ flowing into the second superconductor, and (c) current $I_N(\phi)$ flowing out of the normal-metal lead of a short SNS junction weakly coupled to a normal-metal side probe.

crete levels to zero. In a short SNS junction, this also forces the Josephson current to zero as seen in Fig. 3(b). The variation of current $I_N(\phi)$ flowing out of the normal-metal lead in Fig. 3(c) is also controlled by Andreev energy levels crossing the Fermi level of the normal-metal probe.

The Josephson current flow in a long SNS junction can also be controlled by a normal-metal side probe weakly coupled ($\epsilon=1\%$) to the SNS junction. We plot the Andreev bound levels in a long SNS junction from Eq. (17) in Fig. 4(a), the current I_2 flowing into the second superconductor from Eq. (10) in Figs. 4(b) and 4(c), and the current I_N from Eq. (11) flowing out of the probe is plotted in Fig. 4(d). The supercurrent $I_2(\phi)$ in Figs. 4(b) and 4(c) is again altered from its equilibrium value (dashed) because the effective electrochemical potential $\mu_N=eV$ changes the discrete level occupation. A small current $I_N(\phi)$ from the normal lead also flows into the junction when a new Andreev level falls below the Fermi level of the side probe, as shown in Fig. 4(d).

The lowest Andreev energy level E_0 in a long, ballistic SNS junction,[4] namely,

$$E_0=\frac{\pi\hbar v_F}{L+2\xi_0}, \tag{18}$$

sets the characteristic voltage scale for changes in the current-phase relation. Figures 4(b) and 4(c) shows the current-phase relation for several values of eV/E_0. For electrochemical potential $\mu_{N1}=eV_1=E_0/2$, the phase periodicity of the current $I_2(\phi)$ is halved and its amplitude reduced, as noted in Ref. 7. When $\mu_{N2}=eV_2=E_0$, the current $I_2(\phi)$ is shifted by $\Delta\phi=\pi$, again similar to Ref. 7. Current-phase relations $I_2(\phi)$ intermediate between these two examples are also possible for different applied voltages V. Figure 4(c) shows the Josephson current flowing through the discrete levels being switched off by the bias voltage. For the parameters in Fig. 4 we have $E_0=0.61\Delta$, so for the bias voltage $eV=7E_0/4>\Delta$ in Fig. 4(c) the bound Andreev levels are all filled and carry no net current.

By controlling the discrete level occupation with the side probe voltage, we can directly measure the energy distribution of the Josephson current. The total Josephson current flow is typically broken down into a portion carried by the discrete and continuum levels, namely, $I_2(\phi,V)=I_{2d}(\phi,V)+I_{2c}(\phi,V)$. If we completely populate (or depopulate) all the discrete states with an applied voltage $|eV|\geqslant\Delta$, the total current I_{2d} carried by the bound Andreev levels will be zero, namely $I_{2d}(\phi,|eV|\geqslant\Delta)\simeq 0$. Since the superconducting leads are strongly coupled to the continuum states, while the side probe is only weakly coupled to the states outside the superconducting gap, the portion of the current I_{c2} carried by the energy continuum will be approximately independent of the applied voltage, i.e., $I_{2c}(\phi,V)\simeq I_{2c}(\phi)$. By forcing $I_{2d}(\phi,e|V|\geqslant\Delta)=0$, we should then be able to directly measure the continuum current $I_2(\phi,|eV|\geqslant\Delta)\simeq I_{2c}(\phi)$. This ''continuum current'' is the remaining current which flows when $|eV|\geqslant\Delta$ in Fig. 4(c).

To better understand the energy distribution of the Josephson current in a long SNS junction as a sum of ''discrete'' and ''continuum'' currents, we graph $I_2(\phi,V=0)$ in a long SNS junction having $\epsilon=0$ in Fig. 5. In Fig. 5 the discrete current $I_{2d}(\phi,V=0)$ (dashed) and the continuum current $I_{2c}(\phi,V=0)$ (solid) both contribute to the total current $I_2(\phi,V=0)$ (dot-dashed). Comparing the Josephson current flow when $|eV|\geqslant\Delta$ in Fig. 4(c) to the continuum current in Fig. 5, we see they are identical. The continuum current $I_{2c}(\phi)$ can then be directly measured as a terminal current. Such a measurement should resolve any remaining questions raised in Refs. 4,8,14–16 concerning the energy distribution of the Josephson current between the discrete and continuum energy levels.

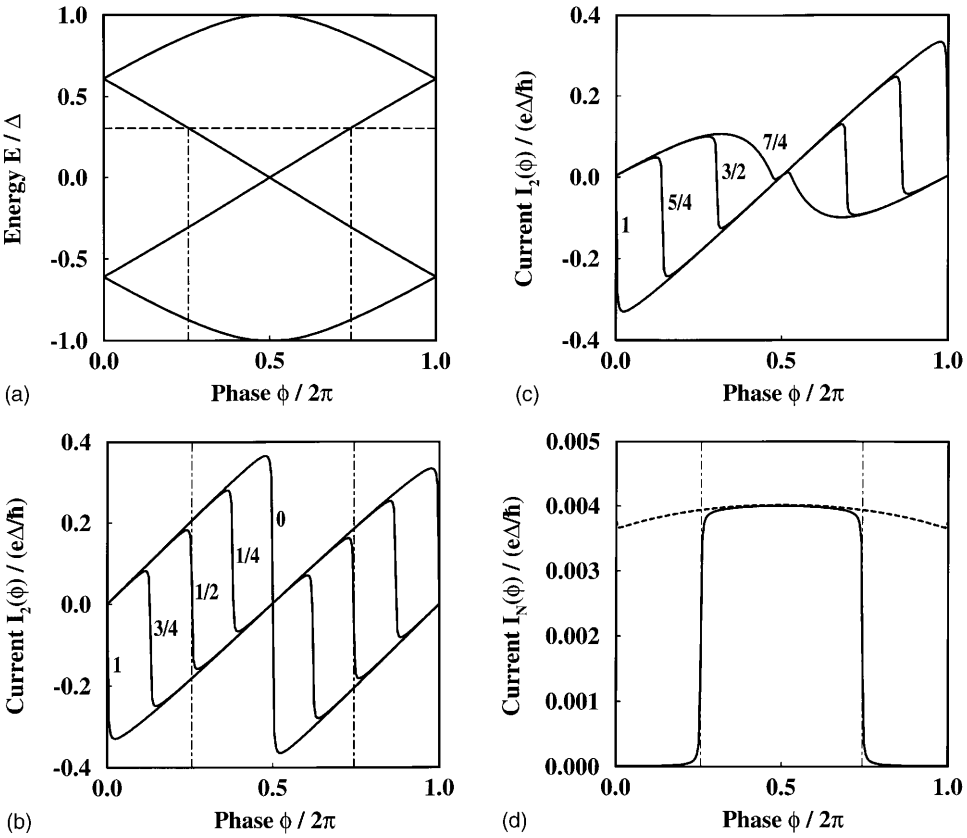

FIG. 4. (a) Andreev energy levels $E_n^{\pm}(\phi)$ for a long SNS junction weakly coupled to a normal-metal side probe. The bias voltage $eV=E_0/2$, where E_0 is the lowest Andreev energy level, is shown by the dotted line. (b) and (c) Current-phase relation $I_2(\phi)$ for different bias voltages eV/E_0. (d) Current $I_N(\phi)$ flowing in from the normal lead when $eV/E_0=1/2$ (solid) and 1 (dashed).

C. Andreev-level spectroscopy and Josephson current switching

The differential conductance $dI_N(\phi,V)/dV$ along the weakly coupled normal-metal lead can also be used to probe the Andreev resonances from Eq. (17). Figure 6 shows the differential conductance in an SNS junction having two Andreev levels for $\epsilon=1\%$(bottom),50,75,100 %(top). When the side probe is weakly coupled, Fig. 6 shows that the differential conductance $dI_N(\phi,V)/dV$ directly detects the Andreev levels. Using Eq. (11) we also find analytically for the $\epsilon\rightarrow 0$ limit in Appendix C that

$$\frac{dI_N}{dV}=\frac{4e^2}{h}\sum_{n,\alpha}\left(\frac{\Gamma_n^2}{\Gamma_n^2+(eV-E_n^{\alpha})^2}\right), \tag{19}$$

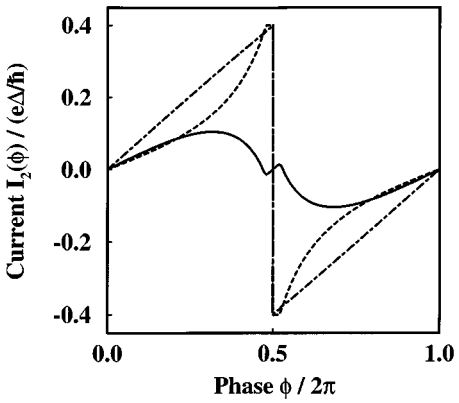

FIG. 5. Current-phase relation $I_2(\phi)$ for a long SNS junction having $eV=0$. The portion of the Josephson current flowing through the continuum energy levels in this isolated ($\epsilon=0$) SNS junction (solid) can be directly measured as a terminal current by applying a voltage $|eV|\geq\Delta$ to a weakly coupled SNS junction, as shown by the curve having $eV=7E_0/4>\Delta$ in Fig. 4(c).

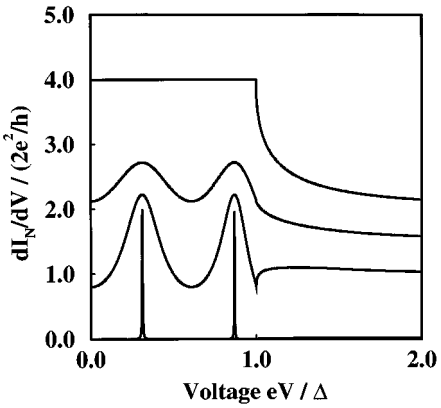

FIG. 6. Differential conductance dI_N/dV ($\phi=\pi/2$) for a long SNS junction containing two Andreev levels. The probe coupling is $\epsilon=1,50,75,100$ %. The Andreev levels appear as sharp peaks in dI_N/dV for $\epsilon=1\%$. The differential conductance dI_N/dV approaches that of a ballistic NS junctions as $\epsilon\rightarrow 100$ %.

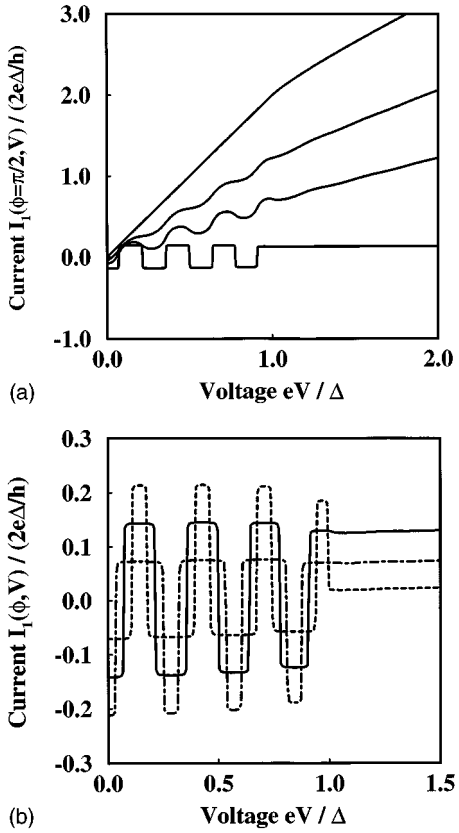

FIG. 7. Current-voltage relation $I_1(\phi=\pi/2,V)$ for a long SNS junction having $L=20\xi_0$. In (a) the coupling strength ϵ = 1, 50, 75, 100 % and $\phi=\pi/2$. I_1 approaches the current-voltage relation for a ballistic NS junction as $\epsilon\rightarrow 100\%$. Switching of the Josephson current I_1 when $|eV|<\Delta$ occurs for the weakly coupled junction ($\epsilon=1\%$). The duty cycle of the switching changes in (b), when the phase difference across the Josephson junction changes. The phase differences in (b) are $\phi=\pi/4$ (dashed), $\phi=\pi/2$ (solid), and $\phi=3\pi/4$ (dot-dashed).

when $|eV|<\Delta$. The resonance width Γ_n in Eq. (19) is $\Gamma_n=\epsilon\Delta[\xi_0/(L+2\xi(E_n)]$, $\xi(E)=\xi_0(\Delta/\sqrt{\Delta^2-E^2})$ is the energy-dependent BCS coherence distance, and the $E_n^{\pm}$ are the Andreev energy-level solutions to Eq. (17). As ϵ increases in Fig. 6, the Andreev resonances apparent in $dI_N(\phi,V)/dV$ become smeared and approach the differential conductance of two ballistic NS junctions[17] in parallel. A possible physical realizaton of this ''Andreev spectrometer'' in is to apply a scanning tunneling microscope (STM) tip[18] to the normal region of an SNS junction. The measurement of the Andreev resonances in SNS junctions using the weakly coupled side probe is similar to the McMillan-Rowell resonances in the I-V relation of an NINS junction.[19]

Varying the probe voltage V also changes the current flow into the superconductors. In Fig. 7(a) we show the current I_2 for another long junction[13] having a fixed phase difference $\phi=\pi/2$. Each graph is for a different coupling strength $\epsilon=1\%(\text{bottom}),50,75,100\,\%(\text{top})$. As the voltage on the normal probe increases, the current $I_2(V)$ corresponding to the weakly coupled probe ($\epsilon=1\%$) in Fig. 7(a) switches abruptly several times when $|eV|\leqslant\Delta$. Each switching of the current in Fig. 7(a) corresponds to another Andreeev level being populated, i.e., when $eV=E_n^{\pm}(\phi)$. As ϵ increases in Fig. 7(a), the current steps round off due to Andreev-level broadening. The current also begins to increase with V, since more current is being admitted from the side probe. When $\epsilon=100\%$ (top), the $I_2(V)$ relation saturates to that of two ballistic NS junctions in parallel.

The switching of the Josephson current in Fig. 7 can be understood more quantitatively using the result from Appendix C, where we find the current flowing inside the superconducting energy gap in the weak-coupling limit $\epsilon\rightarrow 0$ is

$$I_{2d}(\phi,V)=\sum_n \{I_n^-(\phi)f(E_n^-(\phi)-eV) + I_n^+(\phi)f(E_n^+(\phi)-eV)\}. \tag{20}$$

In Eq. (20) the $I_n^{\pm}(\phi)$ are currents carried by the Andreev level n and the voltage eV appears inside the Fermi factors as an effective electrochemical potential. The magnitude of the change in current for each switching event when $\epsilon=1\%$ in Fig. 7 is approximately constant. This constant magnitude of the current change arises because, in a long SNS junction, the currents carried by alternating Andreev energy levels have nearly equal magnitude and opposite signs, namely

$$I_n^{\pm}(\phi)\simeq\mp\frac{ev_F}{L+2\xi_0}. \tag{21}$$

The size of the current step is therefore $\Delta I_1 \simeq\pm ev_F/(L+2\xi_0)$ when $\epsilon=1\%$ in Fig. 7, approximately independent of the phase difference ϕ.

Both the average current and the duty cycle of the switching when $\epsilon=1\%$ depend on the phase difference ϕ, as shown in Fig. 7(b). The continuum current flowing for $|eV|\geqslant\Delta$, when $\epsilon=1\%$ in Fig. 7(b), depends strongly on ϕ. Since the continuum current determines the average or ''background'' current when $\epsilon=1\%$ in Fig. 7(b), the average current depends strongly on ϕ. The ''duty cycle'' for this switching is set by the Andreev-level spacing, which also depends on ϕ. For $\phi=\pi/2$ chosen in Fig. 7(a) the duty cycle is 50%. The phase difference across the SNS Josephson junction can be set using a phase bias network of larger Josephson junctions, as done in Ref. 20.

D. Nonideal junctions

The electrical characteristic discussed here for a one-dimensional, ballistic SNS junctions will be altered if the junction is not ideal. If the superconducting contacts to the SNS junction are not perfectly ballistic, the Josephson current will still display current switching when $e|V|\leqslant\Delta$. However, the magnitude of the change in current will be smaller than for a ballistic SNS junction. If the SNS junction is not purely one-dimensional, the additional available lateral modes will complicate the switching behavior. In the simplest treatment of a wide SNS junction, each mode will conduct independently but with its own Fermi velocity. Consequently, each mode will switch at a different probe (gate) voltage.

Dephasing the quasiparticles with a dephasing time τ_ϕ will only slightly affect the Josephson current switching and Andreev-level spectroscopy discussed in this paper. Al-

though the dephasing time τ_ϕ will increase the Andreev energy-level broadening, the broadened levels will still be filled according to the electrochemical potential of the side probe. Of course the dephasing time must satisfy $v_F\tau_\phi > L+2\xi_0$ for any Josephson effect to exist, whether or not the side probe is present.

Inelastic scattering inside the SNS junction will force the Andreev-level occupation towards the electrochemical potential of the superconductors rather than the electrochemical potential of the side probe,[7] complicating the observation of these effects. In order for the side probe to control the Andreev-level occupation, the lifetime in the Andreev level [see Eqs. (A19) or (C8)] must be shorter than the inelastic-scattering time τ_I, namely $\tau_I > (L+2\xi_0)/v_F\epsilon$ for small ϵ. An electron incident from the side probe must therefore transmit into the SNS junction (couple with some minimum transmission probability $T_{\rm probe} = \epsilon > (L+2\xi_0)/v_F\tau_I$ for the side probe to control the Andreev-level occupation.

The I-V and I-ϕ characteristics described in this paper, however, do not depend on the detailed nature of the weak connection between the SNS junction and a normal-metal probe. Although the probe coupling used in Ref. 7 breaks both the quasiparticle momentum and phase, whereas the probe we employ here breaks only the quasiparticle phase, either type of weakly coupled probe will produce the same I-V characteristics in the weak-coupling limit. As long as the normal-metal probe remains weakly coupled to the Josephson junction, the probe voltage will control the Andreev-level occupation without significantly altering the wave functions and energy-level spectrum of the SNS junction. It should therefore be possible to observe both the switching of the Josephson current described here, and to directly measure the continuum contribution to the Josephson current in a well designed experiment.

IV. CONCLUSIONS

We have solved the BdG equations to calculate the electrical current through an SNS junction coupled to normal-metal side probe. The normal probe models either an STM tip or the gate electrode of a three-terminal SNS junction. The side probe randomizes the quasiparticle phase inside the junction, the same as for normal mesoscopic conductors. But more importantly, a voltage applied to the side probe controls the occupation of the discrete Andreev-levels in the SNS junction, even if the probe is only weakly coupled to the SNS junction. The probe voltage functions an effective Fermi level which controls the Andreev-level occupation. Since a significant portion of the Josephson current flows through the discrete Andreev energy levels, this control of the Andreev-level occupation allows significant control of the Josephson current by changing the voltage of the side probe.

When the side probe is weakly coupled to the SNS junction, the probe voltage can change the Andreev level occupation without significantly altering the wave functions from those of an isolated SNS junction. For a short SNS junction in this weak-coupling limit, we find a finite bias on the side probe can completely switch off the Josephson current as an Andreev level crosses the Fermi level of the probe. In a long SNS junction, we find the Josephson current switches by an amount $\Delta I \simeq ev_F/(L+2\xi_0)$ as the probe voltage varies between $e|V| \lesssim \Delta$. The differential conductance dI_N/dV along the side probe has a peak whenever the Josephson current switches, permitting spectroscopy of the Andreev energy levels. We find also that, with a suitable phase biasing network and when $e|V| \gtrsim \Delta$, one can directly observe the continuum piece of the Josephson current as a terminal current. Some of the unusual current-phase relations predicted here might also be measured in an experiment similar to that of Ref. 21.

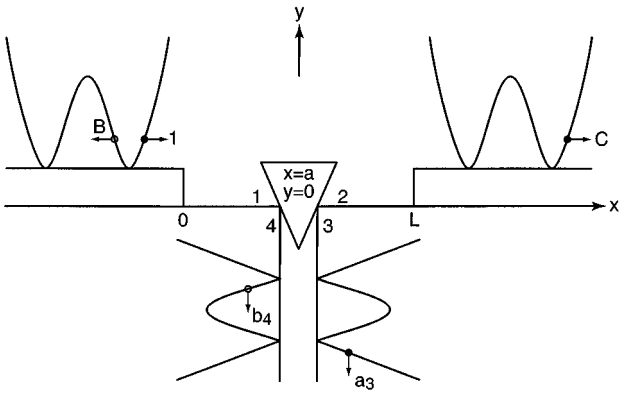

FIG. 8. Scattering state for an electronlike quasiparticle injected from the left superconductor. This injection from lead 1 imposes an electrical current flow in the other leads.

ACKNOWLEDGMENTS

We thank Supriyo Datta for many useful discussions. We gratefully acknowledge financial support from the David and Lucile Packard Foundation and from the National Science Foundation MRSEC program under Grant No. ECS-9201446-01.

APPENDIX A: SCATTERING STATES

To evaluate the electrical current operator in Eq. (5) for the SNS junction coupled to a normal-metal probe, we must first obtain the scattering states for the junction. Consider an electronlike quasiparticle injected from the left superconductor ($x<0$) shown in Fig. 8. In Andreev's approximation, the injected electronlike quasiparticle and the Andreev reflected holelike quasiparticle in the left superconductor ($x<0$) have the wave function

$$\begin{pmatrix} u_0 e^{i\phi_1} \\ v_0 \end{pmatrix} e^{ik_e x} + B \begin{pmatrix} v_0 e^{i\phi_1} \\ u_0 \end{pmatrix} e^{ik_h x}. \tag{A1}$$

We can neglect normal reflections in Eq. (A1), since our coupling to the side probe does not generate normal reflections. The transmitted electronlike quasiparticle in the right superconductor ($x>L$) has the wave function

$$C \begin{pmatrix} u_0 e^{i\phi_2} \\ v_0 \end{pmatrix} e^{ik_e(x-L)}. \tag{A2}$$

The coherence factors u_0 and v_0 in Eqs. (A1) and (A2) are given by Eqs. (15) and (16). The wave vectors k_e and k_h in Eqs. (A1) and (A2) are

$$k_e = \sqrt{\frac{2m}{\hbar^2}(\mu + \sqrt{E^2-\Delta^2})}, \tag{A3}$$

and

$$k_h = \sqrt{\frac{2m}{\hbar^2}(\mu - \sqrt{E^2-\Delta^2})}. \tag{A4}$$

Matching the waves at the pair potential interfaces $x=0$ and $x=L$ allows us to obtain the quasiparticle wave function in the normal region $(0<x<L)$. To the left of the coupler $(0<x<a)$ we have

$$\begin{pmatrix} (Bv_0+u_0)e^{i\phi_1} \\ 0 \end{pmatrix} e^{i\tilde{k}_e x} + \begin{pmatrix} 0 \\ (Bu_0+v_0) \end{pmatrix} e^{i\tilde{k}_h x}, \tag{A5}$$

while, to the right of the coupler $(a<x<L)$, the wave function is

$$\begin{pmatrix} Cu_0 e^{i\phi_2} \\ 0 \end{pmatrix} e^{i\tilde{k}_e(x-L)} + \begin{pmatrix} 0 \\ Cv_0 \end{pmatrix} e^{i\tilde{k}_h(x-L)}. \tag{A6}$$

The wave vectors $\tilde{k}_e$ and $\tilde{k}_h$ in the normal region are calculated from Eqs. (A3) and (A4) with $\Delta=0$.

At $x=a$ and $y=0$ in Fig. 1, the quasiparticle wave amplitudes are connected by a scattering matrix (Refs. 1 and 2) to the normal-metal side probe. The scattering matrix couples the electrical current amplitude j of electrons in the normal region to electrons in the side probe, and holes in the normal region to holes in the side probe by $j_l^{\rm out}=S_{lm}j_m^{\rm in}$, where the lead indices are $l,m=1,2,3,4$. Hence j_1^{out} is the current amplitude flowing out of the coupler in lead 1, etc. We use the same S matrix to independently randomize the phase of both the electrons and holes. Breaking the electron and hole phases in a correlated manner would lead to less energy-level broadening.

In order to break only the phase of quasiparticles without altering their momentum, we couple right-moving quasiparticles in leads 1 and 2 only to lead 3. Left-moving quasiparticles in leads 1 and 2 we allow to scatter only into lead 4. For the scattering matrix we therefore choose[1,2]

$$\mathbf{S} = \begin{pmatrix} 0 & \sqrt{1-\epsilon} & \sqrt{\epsilon} & 0 \\ \sqrt{1-\epsilon} & 0 & 0 & \sqrt{\epsilon} \\ \sqrt{\epsilon} & 0 & 0 & -\sqrt{1-\epsilon} \\ 0 & \sqrt{\epsilon} & -\sqrt{1-\epsilon} & 0 \end{pmatrix}. \tag{A7}$$

The wave function for the electronlike quasiparticle transmitted into lead 3, having a group velocity in the $-y$ direction, is $(y<0)$

$$a_3 \begin{pmatrix} 1 \\ 0 \end{pmatrix} e^{-i\tilde{k}_e y}. \tag{A8}$$

The Andreev reflected holelike quasiparticle, incident on the coupler from lead 2, will produce a transmitted holelike quasiparticle wave function only in lead 4. The wave function for the transmitted holelike quasiparticle in lead 4, which also has a group velocity in the $-y$ direction, is $(y<0)$

$$b_4 \begin{pmatrix} 0 \\ 1 \end{pmatrix} e^{i\tilde{k}_h y}. \tag{A9}$$

The scattering matrix $\mathbf{S}$ from Eq. (A7) relates the current amplitudes for electrons, obtained from Eqs. (A5)–(A9), as

$$\begin{pmatrix} 0 \\ Cu_0 e^{i\phi_2} e^{i\tilde{k}_e(a-L)} \\ a_3 \\ 0 \end{pmatrix} = (\mathbf{S}) \begin{pmatrix} (Bv_0+u_0)e^{i\phi_1}e^{i\tilde{k}_e a} \\ 0 \\ 0 \\ 0 \end{pmatrix}. \tag{A10}$$

The current amplitudes for holes, obtained also from Eqs. (A5)–(A9), are related as

$$\begin{pmatrix} (Bu_0+v_0)e^{i\tilde{k}_h a} \\ 0 \\ 0 \\ b_4 \end{pmatrix} = (\mathbf{S}) \begin{pmatrix} 0 \\ Cv_0 e^{i\tilde{k}_h(a-L)} \\ 0 \\ 0 \end{pmatrix}. \tag{A11}$$

We solve the marix equations in Eqs. (A10) and (A11) to obtain the wave-function amplitudes as

$$B = \left(\frac{v_0}{u_0}\right)[(1-\epsilon)e^{-i\phi}e^{i(\tilde{k}_e-\tilde{k}_h)L}-1]/d, \tag{A12}$$

$$C = \sqrt{1-\epsilon}\left[1-\left(\frac{v_0}{u_0}\right)^2\right]e^{-i\phi}e^{i\tilde{k}_e L}/d, \tag{A13}$$

$$a_3 = \sqrt{\epsilon}u_0\left[1-\left(\frac{v_0}{u_0}\right)^2\right]e^{i\phi_1}e^{i\tilde{k}_e a}/d, \tag{A14}$$

$$b_4 = \sqrt{\epsilon(1-\epsilon)}v_0\left[1-\left(\frac{v_0}{u_0}\right)^2\right]e^{-i\phi}e^{i(\tilde{k}_e-\tilde{k}_h)L}e^{i\tilde{k}_h a}/d, \tag{A15}$$

where

$$d = 1-\left(\frac{v_0}{u_0}\right)^2(1-\epsilon)e^{-i\phi}e^{i(\tilde{k}_e-\tilde{k}_h)L}. \tag{A16}$$

The poles of Eqs. (A12)–(A15) define the quasibound energy levels[19] for right-moving electrons confined inside the SNS junction. By setting $d=0$ from Eq. (A16) we obtain these poles from the solution of

$$1 = \left(\frac{v_0}{u_0}\right)^2(1-\epsilon)e^{-i\phi}e^{i(\tilde{k}_e-\tilde{k}_h)L}. \tag{A17}$$

The right-hand side of Eq. (A17) is the product of probability amplitudes for an electron moving from a NS interface towards the coupler, passing through the coupler, moving towards the other NS interface, Andreev reflecting as a hole, returning to the coupler, passing through the coupler again, propagating back the NS interface, and Andreev reflecting as an electron. The compex energy $E=E_R+iE_I$ which solves Eq. (A17) contains the resonant energy E_R and the lifetime $\hbar/|E_I|$ of the bound level. For energies inside the superconducting gap, Eq. (A17) requires[19]

$$2\pi i n \simeq \ln(1-\epsilon) - 2i\cos^{-1}[(E_R+iE_I)/\Delta] + i[(E_R+iE_I)/\Delta](L/\xi_0) - i\phi. \tag{A18}$$

For very weak coupling ($\epsilon \to 0$), we find the position E_R of the quasibound levels is given by Eq. (17), while the leakage rate $2E_I/\hbar$ is set approximately as

$$-\frac{2E_I}{\hbar} \simeq -\ln(1-\epsilon)\frac{2\Delta\xi_0}{\hbar[L+2\xi(E_R)]} \simeq \epsilon\frac{v_F}{[L+2\xi(E_R)]}. \tag{A19}$$

The leakage rate, which sets the energy level width $|E_I|$, is then simply rate v_F/L at which the quasiparticle encounters the coupler times the probability ϵ of leaking out into the side probe.

APPENDIX B: ELECTRICAL CURRENT

In this appendix, we outline the derivation of the electrical current flowing into the left superconductor. Converting the sum over k into an integral over the injected energies, and making the Andreev approximation, we obtain

$$I_1(\phi,\epsilon,V) = e\left(\int_{-\infty}^{-\Delta} + \int_{\Delta}^{\infty}\right) v_F N_s^+(E)[T_{1;1e}+T_{1;1h}+T_{1;2e}+T_{1;2h}]f(E)dE + e\int_{-\infty}^{\infty} v_F N_n^+(E)[T_{1;3e}+T_{1;4e}]f(E-eV)dE + e\int_{-\infty}^{\infty} v_F N_n^+(E)[T_{1;3h}+T_{1;4h}]f(E+eV)dE, \tag{B1}$$

where the transmission probabilities T are functions of (E,ϕ,ϵ). From the calculation in Appendix A we directly obtain

$$T_{1;1e} = -[1+|B|^2+4u_0v_0\mathrm{Re}B] = -\frac{u_0^4+v_0^4(1-\epsilon)^2+u_0^2v_0^2[(1-\epsilon)^2(1-4v_0^2)+(1-4u_0^2)]}{D(E,\epsilon,-\phi)}, \tag{B2}$$

where $D(E,\epsilon,\phi)$ is defined in Eq. (12). $T_{1;1e}$ is the only transmission coefficient one can directly obtain from the calculation in Appendix A. The other transmission coefficients we find by calculations similar to the one in Appendix A as

$$T_{1;1h} = \frac{u_0^4+v_0^4(1-\epsilon)^2+u_0^2v_0^2[(1-\epsilon)^2(1-4v_0^2)+(1-4u_0^2)]}{D(E,\epsilon,\phi)}, \tag{B3}$$

$$T_{1;2e} = \frac{(1-\epsilon)(u_0^2-v_0^2)^2}{D(E,\epsilon,\phi)}, \tag{B4}$$

$$T_{1;2h} = -\frac{(1-\epsilon)(u_0^2-v_0^2)^2}{D(E,\epsilon,-\phi)}, \tag{B5}$$

$$T_{1;3e} = \begin{cases} \epsilon u_0^2/D(E,\epsilon,\phi); & |E|>\Delta \\ 2\epsilon/F(E,\epsilon,\phi); & |E|<\Delta, \end{cases} \tag{B6}$$

$$T_{1;4e} = \begin{cases} -v_0^2\epsilon(1-\epsilon)/D(E,\epsilon,-\phi); & |E|>\Delta \\ -2\epsilon(1-\epsilon)/F(E,\epsilon,-\phi); & |E|<\Delta, \end{cases} \tag{B7}$$

$$T_{1;3h} = \begin{cases} -\epsilon u_0^2/D(E,\epsilon,-\phi); & |E|>\Delta \\ -2\epsilon/F(E,\epsilon,-\phi); & |E|<\Delta, \end{cases} \tag{B8}$$

$$T_{1;4h} = \begin{cases} v_0^2\epsilon(1-\epsilon)/D(E,\epsilon,\phi); & |E|>\Delta \\ 2\epsilon(1-\epsilon)/F(E,\epsilon,\phi); & |E|<\Delta, \end{cases} \tag{B9}$$

where the function $F(E,\epsilon,\phi)$ is defined in Eq. (13). In Eq. (B1) the factor $N_s^+(E)$ is the superconducting density of states for right-moving quasiparticles, and is related to the normal density of states and $N_n^+(E)$ by

$$N_s^+(E) = \frac{1}{|u_0^2-v_0^2|}N_n^+(E). \tag{B10}$$

Using the identity $v_F N_n^+(E) \simeq 1/h$, and applying Eqs. (B1)–(B10), we obtain

$$I_1(\phi,\epsilon,V)=\frac{e}{h}\left(\int_{-\infty}^{-\Delta}+\int_{\Delta}^{\infty}\right)\frac{f(E)}{|u_0^2-v_0^2|}(2-\epsilon)U(E,\epsilon)\left(\frac{1}{D(E,\epsilon,\phi)}-\frac{1}{D(E,\epsilon,-\phi)}\right)dE$$
$$+\frac{e}{h}\int_{-\Delta}^{\Delta}\left\{\frac{2\epsilon}{F(E,\epsilon,\phi)}-\frac{2\epsilon(1-\epsilon)}{F(E,\epsilon,-\phi)}\right\}f(E-eV)dE-\frac{e}{h}\int_{-\Delta}^{\Delta}\left\{\frac{2\epsilon}{F(E,\epsilon,-\phi)}-\frac{2\epsilon(1-\epsilon)}{F(E,\epsilon,\phi)}\right\}f(E+eV)dE$$
$$+\frac{e}{h}\left(\int_{-\infty}^{-\Delta}+\int_{\Delta}^{\infty}\right)\left\{\frac{u_0^2\epsilon}{D(E,\epsilon,\phi)}-\frac{v_0^2\epsilon(1-\epsilon)}{D(E,\epsilon,-\phi)}\right\}f(E-eV)dE-\frac{e}{h}\left(\int_{-\infty}^{-\Delta}+\int_{\Delta}^{\infty}\right)$$
$$\times\left\{\frac{u_0^2\epsilon}{D(E,\epsilon,-\phi)}-\frac{v_0^2\epsilon(1-\epsilon)}{D(E,\epsilon,\phi)}\right\}f(E+eV)dE. \tag{B11}$$

The function $U(E,\epsilon)$ is defined in Eq. (14). To obtain Eq. (9) from Eq. (B11), apply the identities for the Fermi function $f(E)-f(-E)=2f(E)-1=-\tanh(E/2k_BT)$ to convert the integration over negative energies in Eq. (B11) to run instead over the positive energies. Since the probe breaks only the quasiparticle phase but not its momentum, the current in Eqs. (9)–(11) is independent of the position of the probe ($x=a$).

APPENDIX C: ELECTRICAL CURRENT IN THE WEAK-COUPLING LIMIT

In this appendix we calculate the current $I_2(\phi,V)$ flowing into the right superconductor and the current $I_N(\phi,V)$ flowing out of the normal-metal probe in the weak-coupling limit $\epsilon\to 0$. In taking the $\epsilon\to 0$ limit of Eqs. (9)–(11) one must consider possible resonances inside the integrals, namely, where either $D(E,\epsilon\to 0,\pm\phi)=0$ or $F(E,\epsilon\to 0,\pm\phi)=0$. Resonances in the discrete spectrum occur when the denominator $F(E,\epsilon,\pm\phi)=0$ in Eq. (13), namely the energies where

$$1+(1-\epsilon)^2-2(1-\epsilon)\cos[\theta(E,\pm\phi)]=0. \tag{C1}$$

Here $\theta(E,\pm\phi)$ is the round-trip phase a bound quasiparticle acquires when traversing the SNS junction, namely

$$\theta(E,\phi)=-2\cos^{-1}\left(\frac{E}{\Delta}\right)+\left(\frac{E}{\Delta}\right)\left(\frac{L}{\xi_0}\right)+\phi, \tag{C2}$$

identical to the left-hand side of Eq. (17). Resonances in $F(E,\epsilon\to 0,\pm\phi)=0$ therefore occur when $\theta(E,\pm\phi)=2\pi n$, i.e., at energies equal to the Andreev bound levels in an isolated SNS junction. Consider next possible resonances in the denominator $D(E,\epsilon,\pm\phi)=0$ from Eq. (12), namely, the energies where

$$\frac{u_0^4+v_0^4}{2u_0^2v_0^2}=2\frac{E^2}{\Delta^2}-1=\cos\left[\left(\frac{E}{\Delta}\right)\left(\frac{L}{\xi_0}\right)+\phi\right]. \tag{C3}$$

The only real energy $|E|\geqslant\Delta$ for which Eq. (C3) can be satisfied is at the gap edge, $E=\pm\Delta$, which can be included in the discrete spectrum.

We now turn to the current $I_N(\phi,V)$ flowing out of the normal-metal probe from Eq. (11). Taking the $\epsilon\to 0$ limit of Eq. (11) only the first term survives, namely,

$$-I_N(\phi,\epsilon,V)=\frac{2e}{h}\int_{-\Delta}^{\Delta}\tanh\left(\frac{E-eV}{2k_BT}\right)$$
$$\times\left(\frac{\epsilon^2}{F(E,\epsilon,-\phi)}+\frac{\epsilon^2}{F(E,\epsilon,\phi)}\right)dE. \tag{C4}$$

To expand the integrand near a resonance we write

$$\frac{\epsilon^2}{F(E,\epsilon,\phi)}=\frac{\epsilon^2}{\epsilon^2+2(1-\epsilon)[1-\cos\theta]}\simeq\frac{\epsilon^2}{\epsilon^2+2[1-\cos\theta]}. \tag{C5}$$

Following Ref. 22, we Taylor expand $\cos\theta$ near the resonant energies $E_n^{\pm}$ as

$$[1-\cos\theta(E,\pm\phi)]\simeq\frac{1}{2}[\theta(E,\pm\phi)-2\pi n]^2$$
$$\simeq\frac{1}{2}\left[\frac{d\theta(E,\pm\phi)}{dE}\right]^2(E-E_n^{\pm})^2. \tag{C6}$$

Our approximation for the integrand in Eq. (C4) then becomes

$$\frac{\epsilon^2}{F(E,\epsilon,\pm\phi)}\simeq\frac{\Gamma_{n,\pm}^2}{\Gamma_{n,\pm}^2+(E-E_n^{\pm})^2}, \tag{C7}$$

where the resonance width $\Gamma_{n,\pm}$ is defined as

$$\Gamma_{n,\pm}=\frac{\epsilon}{(\partial\theta(E,\pm\phi)/\partial E)_{E=E_n^{\pm}}}=\frac{\epsilon\Delta\xi_0}{L+2\xi(E_n^{\pm})}. \tag{C8}$$

Since $E_n^+=-E_n^-$, we have $\Gamma_{n,+}=\Gamma_{n,-}\equiv\Gamma_n$. Equation (C8) is therefore the same resonance width obtained from Eq. (A19) in Appendix A, namely, $\Gamma_n=-E_I$.

Substituting Eq. (C7) into Eq. (C4) gives the current I_N flowing out of the normal lead as

$$-I_N(\phi,\epsilon,V)=\frac{2e}{h}\sum_{n,\alpha}\int_{-\Delta}^{\Delta}\left(\frac{\Gamma_n^2}{\Gamma_n^2+(E-E_n^{\alpha})^2}\right)$$
$$\times\tanh\left(\frac{E-eV}{2k_BT}\right)dE, \tag{C9}$$

where $\alpha=-,+$. The differential conductance along the normal lead we can now obtain directly by differentiating Eq. (C9) as

$$\frac{dI_N}{dV}=\frac{2e}{h}\sum_{n,\alpha}\int_{-\Delta}^{\Delta}\left(\frac{\Gamma_n^2}{\Gamma_n^2+(E-E_n^{\alpha})^2}\right)2e\left(-\frac{\partial f(E-eV)}{\partial E}\right)dE. \tag{C10}$$

In the zero-temperature limit, where $-\partial f(E-eV)/\partial E\rightarrow\delta(E-eV)$, the differential conductance provides a means for Andreev energy-level spectroscopy as

$$\frac{dI_N}{dV}=\frac{4e^2}{h}\sum_{n,\alpha}\left(\frac{\Gamma_n^2}{\Gamma_n^2+(eV-E_n^{\alpha})^2}\right). \tag{C11}$$

At finite temperature the differential conductance in Eq. (C11) is thermally broadened by convolving it in energy with the thermal smearing function

$$\left(-\frac{\partial f(E)}{\partial E}\right)=\frac{1}{4k_BT}\mathrm{sech}^2\left(\frac{E}{2k_BT}\right). \tag{C12}$$

The size ΔI_N of the steps in the current along the normal lead are obtained by integrating Eq. (C10) over the voltage (near a resonant level) as

$$\Delta I_N=\int\frac{dI_N}{dV}dV=\epsilon\frac{ev_F}{L+2\xi(E_n)}. \tag{C13}$$

The height of the current steps along the normal lead are then simply the current carried by an Andreev level times the coupling ϵ of the normal lead to the Andreev level.

We now turn to a computation of the current $I_2(\phi,\epsilon\rightarrow0,V)$ flowing into the right superconductor. The current $I_2=I_{2d}+I_{2c}$ again consists of two contributions, I_{2d} from an energy ranges inside and I_{2c} from energies outside the gap. We find from Eq. (10) that current flowing outside the energy gap consists only of a contribution injected from the superconducting leads themselves as

$$I_{2c}(\phi)=\frac{2e}{h}\int_{\Delta}^{\infty}\left[-\tanh\left(\frac{E}{2k_BT}\right)\right]\times|u_0^2-v_0^2|\left(\frac{1}{D(E,-\phi)}-\frac{1}{D(E,\phi)}\right), \tag{C14}$$

where

$$D(E,\phi)=D(E,\epsilon=0,\phi)=u_0^4+v_0^4-2u_0^2v_0^2\cos\left[\left(\frac{E}{\Delta}\right)\left(\frac{L}{\xi_0}\right)+\phi\right]. \tag{C15}$$

Equation (C14) is identical to the continuum piece of the Josephson current calculated in Ref. 8, and is independent of the probe voltage V. Therefore, the weakly coupled probe only controls the discrete current $I_{2d}(\phi,V)$, but does not affect the continuum current $I_{2c}(\phi)$ in the weak-coupling limit.

In the limit $\epsilon\rightarrow0$, the contribution $I_{2d}(\phi,V)$ from the discrete energy spectrum can be written down from Eq. (10) as

$$I_{2d}(\phi,\epsilon,V)=\frac{2e}{\epsilon h}\int_{-\Delta}^{\Delta}\left[-\tanh\left(\frac{E-eV}{2k_BT}\right)\right]\times\left(\frac{\epsilon^2}{F(E,\epsilon,-\phi)}-\frac{\epsilon^2}{F(E,\epsilon,\phi)}\right)dE. \tag{C16}$$

Since $F(E,\epsilon,-\phi)=F(-E,\epsilon,\phi)$, we can write Eq. (C16) as

$$I_{2d}(\phi,\epsilon,V)=\frac{4e}{\epsilon h}\int_{-\Delta}^{\Delta}f(E-eV)\times\left(\frac{\epsilon^2}{F(E,\epsilon,-\phi)}-\frac{\epsilon^2}{F(E,\epsilon,\phi)}\right)dE. \tag{C17}$$

We now apply our Lorentzian approximation for the integrand in Eq. (C17), yielding

$$I_{2d}(\phi,\epsilon,V)\simeq\frac{4e}{\epsilon h}\sum_n\int_{-\Delta}^{\Delta}f(E-eV)\times\left(\frac{\Gamma_n^2}{(E-E_n^-)^2+\Gamma_n^2}-\frac{\Gamma_n^2}{(E-E_n^+)^2+\Gamma_n^2}\right)dE, \tag{C18}$$

where $E_n^{\pm}$ is the Andreev energy described in Eq. (17).

Approximating the Lorentzian functions as δ functions in Eq. (C18), we obtain

$$I_{2d}(\phi,\epsilon,V)\simeq\frac{4e}{\epsilon h}\sum_n\Gamma_n\left[\left(\int_{-\Delta}^{\Delta}\frac{\Gamma_n f(E_n^- -eV)}{(E-E_n^-)^2+\Gamma_n^2}dE\right)-\left(\int_{-\Delta}^{\Delta}\frac{\Gamma_n f(E_n^+ -eV)}{(E-E_n^+)^2+\Gamma_n^2}dE\right)\right]. \tag{C19}$$

The integrations in Eq. (C19) produce

$$\int_{-\Delta}^{\Delta}\frac{\Gamma_n}{(E-E_n^{\pm})^2+\Gamma_n^2}dE=\pi. \tag{C20}$$

The final result for the current flowing into the right superconductor is

$$I_{2d}(\phi,V)=\sum_n\{I_n^-(\phi)f(E_n^-(\phi)-eV)+I_n^+(\phi)f(E_n^+(\phi)-eV)\}, \tag{C21}$$

where

$$I_n^{\pm}(\phi)=\mp\frac{ev_F}{L+2\xi(E_n^{\pm})}. \tag{C22}$$

When $eV=0$, Eq. (C21) reduces to the discrete part of the Josephson current described in Ref. 8. However, for $eV\neq0$ Eq. (C21) shows that the applied voltage on the normal-metal probe is an effective electrochemical potential for the Andreev-level occupation. Equation (C22) is simply the electrical current carried by an Andreev bound level of the isolated Josephson junction[8].

Equation (C21) gives the size of the Josephson current steps produced when a new Andreev level is occupied. When the applied voltage $eV=E_n^-$ the current I_{2d} has a step of size $I_n^-=ev_F/[L+2\xi(E_n^-)]$. When the applied voltage crosses the next Andreev level, namely, $eV=E_n^+$, the current I_{2d} experiences a step of size $I_n^+=-ev_F/[L+2\xi(E_n^+)]$. The current I_{2d} therefore steps alternately up and down as the voltage V varies. Furthermore, these current steps are all approximately the same height. As long as the Fermi level is not too near the gap edge, we can neglect the energy dependence of the coherence distance so that $\xi(E_n^{\pm})\simeq\xi_0$. This analysis yeilds Eq. (21) for the size of the current steps shown in Fig. 7, namely, $\Delta I_2\simeq\pm ev_F/(L+2\xi_0)$. Note that the size of the current steps in I_{2d} are independent of the coupling strength ϵ. The total current I_2 is now

$$I_2(\phi,V)\simeq I_{2d}(\phi,V)+I_{2c}(\phi), \tag{C23}$$

so that the continuum current I_{2c} is simply a background current which sets the dc current level. The discrete current I_{2d} switches as a function of the voltage V, riding on top of the background current level I_{2c}.

[1] M. Büttiker, Phys. Rev. B **32**, 1846 (1985).

[2] M. Büttiker, IBM J. Res. Dev. **32**, 63 (1988).

[3] A.F. Andreev, Zh. Éksp. Teor. Fiz. **46**, 1823 (1964) [Sov. Phys. JETP **19**, 1228 (1964)]; **49**, 655 (1966) [**22**, 455 (1966)].

[4] I.O. Kulik, Zh. Éksp. Teor. Fiz. **57**, 1745 (1969) [Sov. Phys. JETP **30**, 944 (1970)].

[5] C.W.J. Beenakker and H. van Houten, Phys. Rev. Lett. **66**, 3056 (1991).

[6] C.W.J. Beenakker, Phys. Rev. Lett. **67**, 3836 (1991).

[7] B.J. van Wees, K.M.H. Lenssen, and C.J.P.M. Harmans, Phys. Rev. B **44**, 470 (1991).

[8] P.F. Bagwell, Phys. Rev. B **46**, 12 573 (1992).

[9] P.G. deGennes, *Superconductivity of Metals and Alloys* (Addison-Wesley, New York, 1989).

[10] S. Datta, P.F. Bagwell, and M.P. Anantram, Phys. Low Dimens. Struct. **3**, 1 (1996).

[11] P.F. Bagwell, Phys. Rev. B **49**, 6841 (1994).

[12] M. Hurd, S. Datta, and P.F. Bagwell, Phys. Rev. B **54**, 6557 (1996).

[13] All figures use parameters $\mu=100$ meV, $\Delta=0.2$ meV, and $m^*=0.067m_e$. Yielding $\xi_0=11923$ Å and $\lambda_F=150$ Å. Figures 2(a), 2(c), 2(d) and Fig. 3 take $L=0$. Figure 2(b) and Figs. 4, 5, and 6 take $L=3\xi_0$. Figure 7 takes $L=20\xi_0$.

[14] C. Ishii, Prog. Theor. Phys. **44**, 1525 (1970).

[15] J. Bardeen and J.L. Johnson, Phys. Rev. B **5**, 72 (1972).

[16] A.V. Svidzinski, T.N. Antsygina, and E.N. Bratus', Zh. Éksp. Teor. Fiz. **61**, 1612 (1971) [Sov. Phys. JETP **34**, 860 (1972)]; J. Low Temp. Phys. **10**, 131 (1973).

[17] G.E. Blonder, M. Tinkham, and T.M. Klapwijk, Phys. Rev. B **25**, 4515 (1982).

[18] S.H. Tessmer, D.J. van Harlingen, and J.W. Lyding, Phys. Rev. Lett. **70**, 3135 (1993); S.H. Tessmer, M.B. Tarlie, D.J. van Harlingen, D.L. Maslov, and P.M. Goldbart, *ibid.* **77**, 924 (1996).

[19] R.A. Riedel and P.F. Bagwell, Phys. Rev. B **48**, 15 198 (1993); S. Chaudhuri and P.F. Bagwell, *ibid.* **51**, 16 936 (1995).

[20] P. G. N. de Vegvar, T. A. Fulton, W. H. Mallison, and R. E. Miller, Phys. Rev. Lett. **73**, 1416 (1994).

[21] M.C. Koops, G.V. van Duyneveldt, and R. de Bruyn Ouboter, Phys. Rev. Lett. **77**, 2542 (1996).

[22] S. Datta, *Electronic Transport in Mesoscopic Systems* (Cambridge University Press, Cambridge, 1995). See the analysis of single resonant level in Chap. 6.